THE JOURNAL OF PHYSICAL CHEMISTRY B

Article

pubs.acs.org/JPCB

The Influence of Lithium Cations on Dynamics and Structure of Room Temperature Ionic Liquids

Christian Lawler and Michael D. Fayer*

Department of Chemistry, Stanford University, Stanford, California 94305, United States

ABSTRACT: The orientational relaxation dynamics of perylene in the room temperature ionic liquid (RTIL) 1-butyl-3-methylimidazolium bis(trifluoromethyl)sulfonyl imide were studied as a function of lithium ion concentration. Perylene is nonpolar and locates in the alkyl regions of the RTIL. The lithium cation was added as lithium bis(trifluoromethyl)sulfonyl imide, so the addition of Li^+ did not change the anion. The Li^+ concentration ranged from 0 to 0.4 mol fraction. The dynamics were measured by observing the fluorescence anisotropy decay using time correlated single photon counting. The anisotropy experiments and viscosity measurements were performed as a function of temperature for each Li^+ concentration sample. Because perylene has high symmetry, it was possible to independently determine the in-plane and out-of-plane diffusion constants and friction coefficients. With increasing concentration of lithium salt the viscosity increases and both the in-plane and out-of-plane orientational relaxations of perylene become slower. However, the corresponding molecular friction coefficients decreased, with the in-plane coefficient decreasing to a greater extent than the out-of-plane coefficient. The decrease in the friction coefficients demonstrates that lithium ions, which are located in the ionic regions of the RTILs, change the structure of the alkyl regions of the RTIL.

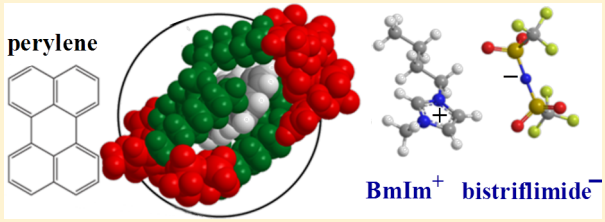

I. INTRODUCTION

Room temperature ionic liquids (RTIL) have attracted significant interest for their distinctive physical properties and for a number of potential applications, such as use as solvents for chemical reactions[1] and as electrolytes for lithium-ion batteries.[2] RTILs may have a number of advantages in the latter application,[3,4] such as broad electrochemical windows, nonflammability, and negligible vapor pressure, which helps avoid the fire and explosion risks associated with volatile organic solvents used in conventional lithium-ion batteries.

Relative to the neat liquids, the viscosities of solutions of lithium salts in RTILs increase significantly.[5,6] The results of experimental studies[7−9] and molecular dynamics simulations[8−10] suggest that RTIL anions aggregate around the Li^+ ions, producing the increase in viscosity. Because of the importance of lithium ion transport to battery operation, the influence of lithium ions on RTIL structure and dynamics is a topic of interest.

The alkylimidazolium bistriflimide ionic liquids are attractive for battery applications because of their relatively low viscosities, as well as good electrochemical stability[4] and broad operating temperature ranges. Many organic RTILs display nanoscale liquid structure, with the anions and charged head groups of the cations forming hydrophilic regions distinct from the hydrophobic regions formed by the alkyl tails of the cation.[11−17] A large number of experiments conducted on RTILs, including fluorescence,[18−21] optical Kerr effect,[22−28] and dielectric spectroscopies;[25,29] NMR;[30,31] small-angle X-ray scattering (SAXS);[32] and small-angle neutron scattering (SANS),[33] have been interpreted in the context of a structured liquid segregated into ionic and organic regions. 1-Butyl-3-methylimidazolium bis(trifluoromethyl)sulfonyl imide ([BmIm][Tf_2N]) is a well-studied liquid with a sufficiently long cation alkyl group for the RTIL to exhibit nanostructured organization into distinct hydrophobic and hydrophilic regions,[21] while having a lower viscosity than alkylimidazolium RTILs with longer cation alkyl chains.

Perylene is a hydrophobic polyaromatic hydrocarbon which can serve as a fluorescent probe of the alkyl regions of RTILs.[21] Figure 1 shows the structure of perylene; the transition dipole for the $S_1 \rightarrow S_0$ emission transition lies along the long axis of the molecule (the *x*-axis in the coordinate system used here).

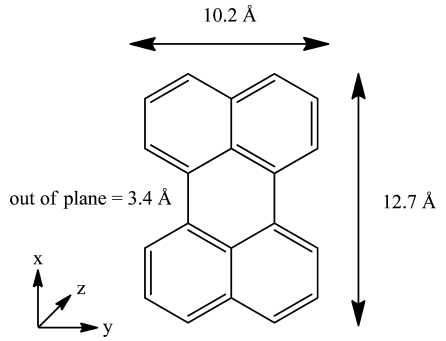

Figure 1. Perylene structure and dimensions. Rotation about the *z*-axis is in-plane. Rotation about the *y*-axis is out of plane.

Received: June 10, 2013
Revised: July 19, 2013
Published: July 23, 2013

Detailed studies of perylene in a series of RTILs with the bistriflimide anion and the imidazolium cation with different chain lengths establish that perylene is located in the hydrocarbon regions of the liquids,[21,34] consistent with studies on the solvation of nonpolar solutes in alkylimidazolium-based ionic liquids.[35,21,34] In addition, a study of a similar fluorescence probe, 9-phenylanthracene, in 3-octyl-1-methylimidazolium bistriflimide, including NMR experiments, establishes that large polycyclic aromatic hydrocarbons locate in hydrocarbon regions of the RTILs.[36] This is in contrast to much smaller single-ring aromatics that may possibly locate in the ionic region because of π-stacking interactions.[37−39] Thus, perylene's orientational dynamics report specifically on the local environment in the RTIL alkyl region. Changes in the orientational dynamics and the friction coefficients obtained from the measurements as a function of lithium cation concentration will reflect changes in the local structure of the RTIL.

In this study, perylene was dissolved in [BmIm][Tf_2N] with various concentrations of lithium salt, in the form of lithium bis(trifluoromethyl)sulfonyl imide ($LiTf_2N$) so that the RTIL anion was unchanged. The fluorescence anisotropy decay of perylene was measured by the technique of time-correlated single photon counting as a function of temperature for each solution. From the measurements, the perylene orientational diffusion constants for reorientation both in and out of the plane of the molecule were obtained. Temperature-dependent viscosities were also measured for each Li^+ concentration, which allowed the orientational friction coefficients for perylene in each solution to be determined. It was found that as the lithium ion concentration increased, the friction coefficients for both in-plane and out-of-plane rotations decreased below the theoretical value for slip boundary conditions, indicating the presence of a complex solvation structure in the vicinity of perylene that changes with lithium concentration.

II. EXPERIMENTAL PROCEDURES

Samples of [BmIm][Tf_2N] were obtained from IoLiTec corporation. Before use, the samples were heated under vacuum at 60 °C for 24 h to dry, after which their water concentration was measured by Karl Fischer titration and found to be very low, < 100 ppm. $LiTf_2N$ was obtained from Sigma Aldrich and used as received. All chemicals were stored and handled in a glovebox under a dry nitrogen atmosphere.

Temperature-dependent dynamic viscosities were measured for each ionic liquid/lithium salt solution using a Brookfield Engineering LV-DV II+ Pro rotary cone−plate viscometer. The viscometer was located in the glovebox to prevent the uptake of water during the viscosity measurements.

[BmIm][Tf_2N] solutions were prepared with $LiTf_2N$ mole fraction, $\chi(LiTf_2N)$, of 0, 0.1, 0.15, 0.2, 0.3, and 0.4. Sufficient perylene was dissolved in each sample to give an absorbance of 0.3 at 405 nm. The samples were contained in 2 mm path length sealed sample cells for use in the fluorescence experiments.

The time-dependent fluorescence anisotropy was measured using the time-correlated single photon counting (TCSPC) technique. The excitation source was a Ti:sapphire oscillator, which produced ~100 fs pulses at a rate of 80 MHz, reduced to 4 MHz with an acousto-optic single-pulse selector. The oscillator wavelength was set to 810 nm, which was then doubled to 405 nm with a beta-barium oxide doubling crystal. After passing through a half-wave plate that enabled rotation of the polarization of the excitation beam, the laser pulses at 405 nm were used to excite the sample. The collected fluorescence from the sample was passed through a fixed polarizer mounted on the entrance slit of a monochromator while the polarization of the excitation beam was rotated among fixed angles to measure time-dependent fluorescence parallel, perpendicular, and at the magic angle relative to the polarization of the excitation beam. Fluorescence was detected at 469 nm. Measurements were made for each sample at a series of temperatures between 298 and 333 K.

The instrument response was measured using a solution of malachite green in ethanol. Malachite green in ethanol has an ~5 ps fluorescence lifetime,[40] which is so short it does not contribute to the measured instrument response. The absorbance of the malachite green sample was matched to the absorbance of the perylene samples at 405 nm. The instrument response sample was contained in the same sample cell and placed in the same sample position as used in the anisotropy experiments. The instrument response was less than 70 ps in all cases.

III. RESULTS AND DISCUSSION

The experiment measures $I_{\parallel}(t)$ and $I_{\perp}(t)$, the intensity of fluorescence from the sample collected with parallel and perpendicular polarization, respectively, relative to the excitation beam. The anisotropy is defined in terms of $I_{\parallel}(t)$ and $I_{\perp}(t)$ as

$$r(t) = \frac{I_{\parallel}(t) - I_{\perp}(t)}{I_{\parallel}(t) + 2I_{\perp}(t)} \tag{1a}$$

The population relaxation, $P(t)$, is given by

$$P(t) = I_{\parallel}(t) + 2I_{\perp}(t) \tag{1b}$$

In eq 1a, the denominator divides out the population relaxation contribution. Therefore, $r(t)$ is a measure of the orientational relaxation only.

Figure 2 shows a representative time-dependent fluorescence anisotropy plot (black curve), for perylene in a [BmIm][Tf_2N] solution with $\chi(LiTf_2N)$ = 0.2 at 298 K. The red curve is a biexponential fit to the data. The fit is started at 200 ps, after the instrument response no longer affects the data. The

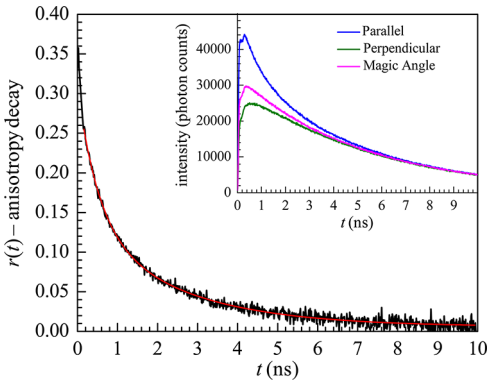

Figure 2. Time-dependent fluorescence anisotropy decay $r(t)$ (black curve) and the fit to the data (red curve) for perylene in a 0.2 mol fraction solution of $LiTf_2N$ in [BmIm][Tf_2N] at T = 298 K. The inset shows time-dependent fluorescence intensity for fluorescence polarized parallel (blue curve), at the magic angle (pink curve), and perpendicular (green curve) to the polarization of the excitation source.

dx.doi.org/10.1021/jp405752q | J. Phys. Chem. B 2013, 117, 9768−9774

dynamics that are measured are slow enough that it is not necessary to use the instrument response and convolutions to obtain the desired data. Similar anisotropy data were collected for each lithium concentration at a series of temperatures.

In terms of the dynamical variables of orientational diffusion, the anisotropy is given by[41]

$$r(t) = \frac{6}{5}(q_y q_z \gamma_y \gamma_z e^{-3(D_x+D)t} + q_x q_z \gamma_x \gamma_z e^{-3(D_{yx}+D)t} + q_x q_y \gamma_x \gamma_y e^{-3(D_z+D)t}) + \frac{3}{10}((\beta+\alpha)e^{-(6D+2\Delta)} + (\beta-\alpha)e^{-(6D-2\Delta)}) \quad (2)$$

where D_i is the diffusion constant for rotation of perylene about its ith axis, and q_i and γ_i are the projections of the excitation and emission dipoles, respectively, onto that axis. The quantities α, β, D, and Δ are given by

$$\alpha = \frac{1}{\Delta}[D_x(q_y^2\gamma_y^2 + q_z^2\gamma_z^2 - 2q_x^2\gamma_x^2 + q_x^2 + \gamma_x^2) + D_y(q_x^2\gamma_x^2 + q_z^2\gamma_z^2 - 2q_y^2\gamma_y^2 + q_y^2 + \gamma_y^2) + D_z(q_x^2\gamma_x^2 + q_y^2\gamma_y^2 - 2q_z^2\gamma_z^2 + q_z^2 + \gamma_z^2) - 2D] \quad (3)$$

$$\beta = q_x^2\gamma_x^2 + q_y^2\gamma_y^2 + q_z^2\gamma_z^2 - \frac{1}{3} \quad (4)$$

$$D = \frac{1}{3}(D_x + D_y + D_z) \quad (5)$$

$$\Delta = (D_x^2 + D_y^2 + D_z^2 - D_xD_y - D_xD_z - D_yD_z)^{1/2} \quad (6)$$

Because of perylene's D_{2h} symmetry, and the alignment of the absorption and emission dipoles with a principal axis of the molecule, the expression for its anisotropy can be reduced to a sum of two exponentials. By making the simplifying approximation of treating perylene as an oblate spheroid (for which $D_x = D_y \ll D_z$), the general anisotropy in (2) can be simplified to

$$r(t) = 0.1e^{-(2D_y+4D_z)t} + 0.3e^{-D_y t} \quad (7)$$

In practice, ultrafast inertial orientational relaxation causes perylene to have a lower than the ideal initial $t = 0$ anisotropy of 0.4;[42] the values of the numerical coefficients in eq 7 are always found to be less than the theoretical values and are obtained in the fits to the data.

The orientational diffusion constants are obtained from the experimental data by first fitting the experimental anisotropy with a sum of two exponentials:

$$r(t) = A_1e^{-t/\tau_1} + A_2e^{-t/\tau_2} \quad (8)$$

Using eqs 7 and 8, the diffusion constants D_y (rotation out of the plane of the molecule around the y axis) and D_z (rotation in the plane of the molecule around the z axis) can be found algebraically in terms of τ_1 and τ_2 from the fits. We take the out of plane orientational diffusion, D_y, to be associated with slow component in the biexponential anisotropy decay because the out of plane motion requires sweeping out more volume than the in plane component, D_z. Therefore, D_y is obtained from τ_2, the slow decay component, and D_z is obtained from τ_1, the fast decay component and eq 7. In addition, the average diffusion constant, D, is obtained from eq 5. To show the nature of the trends with Li^+ concentration, the three diffusion constants are displayed for a single temperature, 298 K, in Figure 3. The dashed lines are aids to the eye. With the exception of the points at $\chi = 0.1$, the points all fall very close to the lines. The points for $\chi = 0.1$ are probably off the lines because of experimental error, but we cannot rule out the possibility that the diffusion constants do not change in a linear manner with Li^+ mole fraction. As is clear from the figure, the orientational diffusion becomes slower with increasing lithium ion concentration. Orientational diffusion constants for solute molecules generally depend inversely on solution viscosity, and the viscosity of [BmIm][Tf_2N] solutions increase with $LiTf_2N$ concentration, as shown in Figure 4. The temperature-dependent viscosities fit very well with single exponentials with a small offset (R^2 greater than 0.999 for each $LiTf_2N$ concentration). The parameters for the exponential fits are given in Table 1 so that the viscosity over the range of temperatures studied can be obtained for the various Li^+ concentrations.

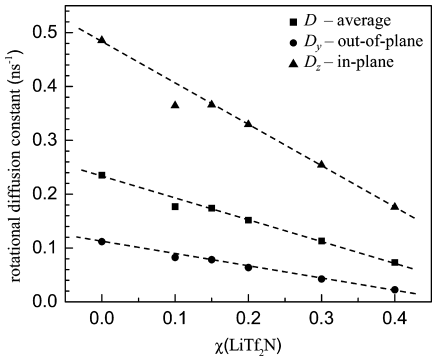

Figure 3. Orientational diffusion constants for perylene in [BmIm][Tf_2N] solutions at 298 K with various $LiTf_2N$ mole fractions.

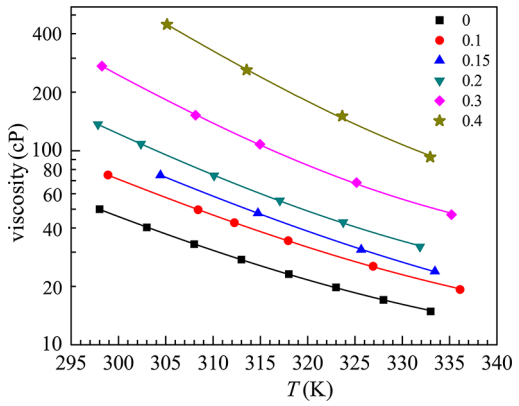

Figure 4. Temperature-dependent viscosities of [BmIm][Tf_2N] solutions with $\chi(LiTf_2N) = 0$ to 0.4. The y-axis is presented on a natural log scale. Lines connecting the data points are single exponential fits to the data. The parameters for the lines are given in Table 1.

For orientational diffusion that follows hydrodynamic behavior, the orientational diffusion constant, D, and reorientation time τ for a solute depend on the temperature and viscosity of the solution according to

$$\tau = \frac{1}{6D} \propto \frac{\eta}{kT} \quad (9)$$

dx.doi.org/10.1021/jp405752q | J. Phys. Chem. B 2013, 117, 9768−9774

Table 1. Parameters of Single Exponential Fits, $\eta = Ae^{-mT} + b$, to Viscosities of $LiTf_2N$/[BmIm][Tf_2N] Solutions as Functions of Temperature

lithium ion mole fraction	A	m	b
0	1.7×10^8	20	8.0
0.1	2.9×10^8	20	9.7
0.15	4.9×10^8	19	9.4
0.2	4.5×10^9	17	16
0.3	1.2×10^{11}	15	27
0.4	1.2×10^{12}	14	38

Here, the orientational diffusion constant, D, is the average of the diffusion constants D_x, D_y, and D_z from eq 5. η is the dynamic viscosity of the solution, k is Boltzmann's constant, and T is the absolute temperature.

In Figure 5, the experimental values of τ taken over a range of temperatures for perylene for each lithium/RTIL solution

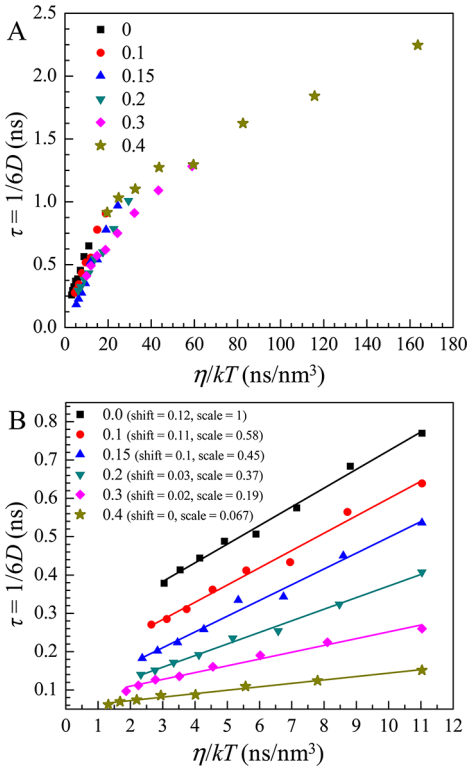

Figure 5. Orientational relaxation times, $\tau = {}^1/_6D$, (symbols) for perylene plotted against the dynamic viscosity η over kT, for $\chi(LiTf_2N) = 0$ to 0.4. The raw data are presented in A. In B the plots are scaled and shifted vertically by the values given in the inset to aid visual comparison. The slopes of the plots have been preserved in each case. The lines through the data points are linear least-squares fits to the data and show that the orientational diffusion is hydrodynamic.

are plotted against η/kT. Figure 5A shows all of the data with a single set of axes. To make it easier to see the nature of the results and the trends, Figure 5B shows the same plots rescaled and shifted. The true slopes of the data, which represent the proportional dependence of τ on η/kT, have been preserved in all cases. Linear least-squares fits gave an R^2 of greater than 0.98 for each sample. The linearity of the plots confirms hydrodynamic behavior. To obtain actual values of τ for the corresponding η/kT from Figure 5B, find the point of interest on the plot and the associated shift and scale values from the inset. Subtract the shift value from τ and then divide both τ and η/kT by the scale factor.

As can be seen in Figures 3 and 5, as the mole fraction of Li^+ increases the diffusion constants become slower (the orientational relaxation time constants become longer). This is expected as increasing $\chi(LiTf_2N)$ increases the viscosity at any given temperature. However, to determine whether the slower orientational diffusion of perylene with increasing lithium ion concentration is solely a consequence of increasing viscosity or indicates a structural change in perylene's solvation environment, it is necessary to analyze the trends in the diffusion constants with temperature and viscosity. A useful approach is to consider the unitless friction coefficient C, which represents the coupling between the solute and the solvent and is independent of temperature and viscosity for rotators that display hydrodynamic behavior.[43,44] Figure 5B shows that the orientational relaxation of perylene in all of the samples is hydrodynamic. The friction coefficient C_i for rotation about the ith axis of an oblate ellipsoid is related to the associated D_i as[43]

$$C_i = \frac{kT}{\eta V D_i} \tag{10}$$

where V is the volume of the solute. C_i can be calculated from the measured temperature-dependent values of D_i and η. For perylene in each solution, Table 2 gives the ratios of the

Table 2. Ratios of In-Plane and Out-of-Plane Friction Coefficients to Their Theoretical Slip Values

lithium ion mole fraction	in-plane	out-of-plane
0	1.70	0.512
0.1	1.64	0.480
0.15	1.23	0.371
0.2	1.08	0.336
0.3	0.597	0.228
0.4	0.264	0.160

experimental in-plane and out-of-plane friction coefficients to their theoretical slip values, which can be calculated from the dimensions of the rotator.[43,45] Figure 6 is a plot of the friction coefficients with a linear fit to the data points. The friction coefficients change significantly with lithium ion concentration. The fact that the coupling between solute and solvent, as quantified by the friction coefficients, is not constant with $LiTf_2N$ concentration demonstrates that adding lithium ions

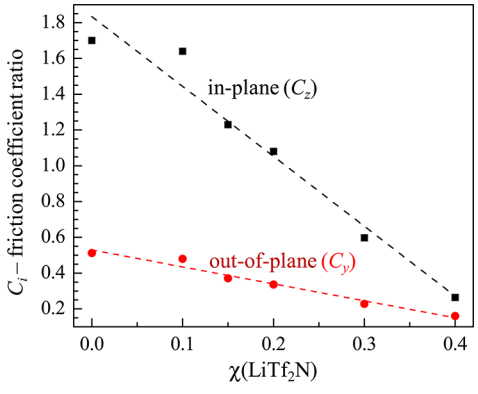

Figure 6. The in-plane and out-of-plane friction coefficient ratios as a function of lithium cation concentration.

dx.doi.org/10.1021/jp405752q | J. Phys. Chem. B 2013, 117, 9768–9774

has an effect on the alkyl region of the RTIL beyond altering the solutions' bulk viscosities. As shown in Table 2 and can be seen in Figure 6, both in-plane and out-of-plane orientational friction coefficients decrease as the Li^+ concentration increases. The in-plane friction coefficient (C_z) is greater than the theoretical slip value with no lithium cations in the solution. As $LiTf_2N$ is added, the in-plane friction coefficient falls, becoming subslip for concentrations above $\chi(LiTf_2N) = 0.2$. The out-of-plane friction coefficient (C_y) is subslip even for $\chi = 0$. It becomes increasingly subslip as $\chi(LiTf_2N)$ increases. C_z decreases more in relative terms than does C_y; C_z decreases by a factor of ~6 from $\chi(LiTf_2N) = 0$ to 0.4, while C_y decreases by a factor of ~3. At high lithium ion concentration, $\chi(LiTf_2N) = 0.4$, C_z is approaching C_y.

The decreases in the friction coefficients, C_z and C_y, show that changes in the liquid structure in the RTIL alkyl region in response to increased lithium concentration result in less hindered orientational diffusion both in and out of the plane of perylene after adjusting for the increased viscosity of the RTIL. This is in contrast to the effect of increasing alkyl chain length on perylene in 1-alkyl-3-methylimidazolium bistriflimides. Previous work[21] found that as the length of the cation's alkyl tail increased, the dynamics of the perylene probe converged toward those of an ordered alkane, with the in-plane C_z (rotation about the z axis) decreasing and becoming subslip while the out-of plane C_y (rotation about the y axis) increased. Therefore, the structural changes in the alkyl region in response to lithium ions are qualitatively different from those that result from changing the alkyl chain length.

The trends in the orientational dynamics of perylene can provide insights into the changing nature of the liquid structure of the RTIL alkyl regions as lithium cation is added. Slip boundary conditions for orientational diffusion of solute molecules apply when the interactions with the solvent are not strong, for instance, no solute−solvent hydrogen bonding. Slip boundary conditions are frequently seen for solvents that are similar in size or larger than the solute molecules.[46] Under these conditions, the rotating solute does not "drag" solvent with it. A hypothetical spherical solute with slip boundary conditions would rotate freely. However, for nonspherical solutes with slip boundary conditions, the solute must still displace solvent molecules that are within its swept volume as it rotates, which gives rise to the friction. In some cases, C may be less than the theoretical slip value; such subslip behavior has generally been explained by the presence of void spaces or excess free volume in the local liquid structure around the rotator, giving lower than average solvent density within the swept volume of the rotating solute.[47−49]

Table 2 and Figure 6 show that for the pure liquid (no Li^+), the in-plane friction is greater than the out-of-plane friction. As discussed above, the numbers in Table 2 and Figure 6 are the ratios of the measured friction coefficients to the theoretical values for perylene modeled as an oblate ellipsoid. A value of 1 means the measured friction coefficient is the same as the value for the perylene model under slip conditions. The slip condition can be thought of as occurring with a hypothetical ideal solvent that does not have a particular local structure that is different for in-plane and out-of-plane. The only source of friction is sweeping out the volume of solvent molecules by the rotator. The model oblate ellipsoid in this ideal solvent would have friction coefficient ratios in-plane and out-of-plane that are both 1. The fact that the in-plane ratio is greater than slip and substantially larger than the out-of-plane ratio, which is subslip, indicates that perylene finds itself in a structured environment even in the absence of lithium cation. The structure is such that relative to the theoretical slip calculation, it is more difficult for perylene to push the alkyl tails of the RTIL out of the way when rotating in the plane of the molecule than out of the plane. This is in contrast to perylene embedded in the alkyl chains of paraffin oil for which the two friction coefficients ratios are almost identical and both are subslip.[21]

Table 2 and Figure 6 show that increasing the Li^+ concentration causes both friction coefficient to decrease. These decreases as $\chi(LiTf_2N)$ increases clearly demonstrate that putting Li^+ in the ionic regions of the RTIL changes the structure of the alkyl regions. It is becoming easier for perylene to undergo rotational diffusion (after accounting for the increased viscosity of the solutions) as the Li^+ concentration increases. The change is more pronounced for the in-plane motion than the out-of-plane motion, and both motions become substantially subslip at $\chi(LiTf_2N) = 0.4$. Adding Li^+ to the ionic region can change its organization causing the configuration of the BmIm cations to alter as the Li^+ concentration grows. Changing the configuration of imidazolium cations in the ionic regions apparently alters the organization of the butyl chains that solvate perylene in the alkyl regions. The large decrease in the friction coefficients implies that the chain packing density around the perylene is reduced, but in an anisotropic manner. The structuring in the ionic regions may generate a good deal of free volume in the alkyl regions, resulting in reduced hindrance of perylene orientational diffusion.

Both Raman[7] and optical heterodyned detected optical Kerr effect[27] experiments have indicated a change in the nature of $LiTf_2N$ solvation by $[BmIm][Tf_2N]$ at $\chi(LiTf_2N) = 0.2$. The Raman results have been interpreted as showing that lithium ions are solvated by approximately 2 $[Tf_2N]^-$ per Li^+ at $\chi(LiTf_2N) < 0.2$, with a change to solvation by ~4 anions above $\chi(LiTf_2N) = 0.2$.[7] MD simulations also show a change in the solvation of Li^+ as the Li^+ concentration is increased.[10] However, a recent MD simulation study finds that there is no substantial change in the number of anions solvating Li^+ as the lithium ion concentration is increased.[50] If there is an abrupt change in solvation of Li^+ at $\sim\chi(LiTf_2N) = 0.2$, it is not manifested in the perylene orientational relaxation data shown in Figure 6. Within experimental error, the changes in the friction coefficient ratios is continuous with $\chi(LiTf_2N)$, suggesting a continuous change in the arrangement of the imidazolium cations.

IV. CONCLUDING REMARKS

The temperature-dependent orientational diffusion of perylene in solutions of $LiTf_2N$ in $[BmIm][Tf_2N]$ was studied as a function of the Li^+ concentration by time-dependent fluorescence anisotropy measurements. Orientational diffusion constants D_i were determined for perylene as functions of temperature and lithium ion concentration and were found to follow hydrodynamic behavior. The ratios of the experimental orientational friction coefficients to the theoretical friction coefficients of an oblate ellipsoid with slip boundary condition were calculated for both in-plane and out-of-plane reorientation of perylene in each of the solutions. The in-plane friction coefficient ratio is always greater than the out-of-plane ratio, with both decreasing substantially with increasing lithium concentration. The decrease in the friction coefficients with increasing Li^+ concentration (see Figure 6) demonstrates that

dx.doi.org/10.1021/jp405752q | J. Phys. Chem. B 2013, 117, 9768−9774

decrease in the measured orientational diffusion constants as Li^+ concentration increases (see Figure 3) is not caused solely by an increase in the solutions' bulk viscosities.

The in-plane and out-of-plane friction coefficients are significantly different at all Li^+ concentrations, demonstrating anisotropic solvation of perylene in the alkyl regions of the RTIL. At high Li^+ concentrations, both the in-plane and out-of-plane friction coefficients are subslip. It is posited that the decreases in the friction coefficients with increasing Li^+ concentration is caused by changes in the arrangement of the imidazolium cations, which in turn forces changes in the alkyl chain organization in the organic regions of the RTIL. The substantially subslip orientational friction coefficients at high Li^+ concentration suggest a reduction of the alkyl chain packing around the perylene, with the reduction being greater in-plane than out-of-plane.

Tiwari and co-workers found that the rate of an intramolecular Diels–Alder reaction involving a nonpolar reactant does not change significantly in going from $BmIm^+Tf_2N^-$ to $BmIm^+BF_4^-$, even though the viscosity changes substantially.[51] The reaction involves the rotation of the dienophile over the plane of the molecule. This is the direction of rotation in [BmIm][Tf_2N] that is most strongly subslip. Figure 6 shows that the addition of $LiTf_2N$ to [BmIm][Tf_2N] changes the in-plane and out-of-plane friction coefficients to a different extent. It is interesting to speculate that in an RTIL like $BmImTf_2N$ a chemical reaction dependent on anisotropic motions in an alkane could be modified by tuning the anisotropy in the alkyl region of the RTIL with the Li^+ concentration in the ionic region.

AUTHOR INFORMATION

Corresponding Author

*E-mail: fayer@stanford.edu.

Notes

The authors declare no competing financial interest.

ACKNOWLEDGMENTS

This work was funded by the Division of Chemistry, Directorate of Mathematical and Physical Sciences, National Science Foundation Grant No. CHE-1157772.

REFERENCES

(1) Sureshkumar, M.; Lee, C.-K. Biocatalytic Reactions in Hydrophobic Ionic Liquids. *J. Mol. Catal. B, Enzym.* **2009**, *60*, 1–12.

(2) Hagiwara, R.; Lee, J. S. Ionic Liquids for Electrochemical Devices. *Electrochemistry* **2007**, *75*, 23–34.

(3) Lewandowski, A.; Świderska-Mocek, A. Ionic Liquids as Electrolytes for Li-Ion Batteries—an Overview of Electrochemical Studies. *J. Power Sources* **2009**, *194*, 601–609.

(4) Galiński, M.; Lewandowski, A.; Stępniak, I. Ionic Liquids as Electrolytes. *Electrochim. Acta* **2006**, *51*, 5567–5580.

(5) Takada, A.; Imaichi, K.; Kagawa, T.; Takahashi, Y. Abnormal Viscosity Increment Observed for an Ionic Liquid by Dissolving Lithium Chloride. *J. Phys. Chem. B* **2008**, *112*, 9660–9662.

(6) Vega, J. A.; Zhou, J.; Kohl, P. A. Electrochemical Comparison and Deposition of Lithium and Potassium from Phosphonium- and Ammonium-Tfsi Ionic Liquids. *J. Electrochem. Soc.* **2009**, *156*, A253–A259.

(7) Duluard, S.; Grondin, J.; Bruneel, J.-L.; Pianet, I.; Grélard, A.; Campet, G.; Delville, M.-H.; Lassègues, J.-C. Lithium Solvation and Diffusion in the 1-Butyl-3-Methylimidazolium Bis-(Trifluoromethanesulfonyl)Imide Ionic Liquid. *J. Raman Spectrosc.* **2008**, *39*, 627–632.

(8) Monteiro, M. J.; Bazito, F. F. C.; Siqueira, L. J. A.; Ribeiro, M. C. C.; Torresi, R. M. Transport Coefficients, Raman Spectroscopy, and Computer Simulation of Lithium Salt Solutions in an Ionic Liquid. *J. Phys. Chem. B* **2008**, *112*, 2102–2109.

(9) Umebayashi, Y.; Hamano, H.; Seki, S.; Minofar, B.; Fujii, K.; Hayamizu, K.; Tsuzuki, S.; Kameda, Y.; Kohara, S.; Watanabe, M. Liquid Structure of and Li+ Ion Solvation in Bis-(Trifluoromethanesulfonyl)Amide Based Ionic Liquids Composed of 1-Ethyl-3- Methylimidazolium and *N*-Methyl-*N*-Propylpyrrolidinium Cations. *J. Phys. Chem. B* **2011**, *115*, 12179–12191.

(10) Borodin, O.; Smith, G. D.; Henderson, W. Li^+ Cation Environment, Transport, and Mechanical Properties of the LiTFSI Doped *N*-Methyl-*N*-Alkylpyrrolidinium+TFSI-Ionic Liquids. *J. Phys. Chem. B* **2006**, *110*, 16879–16886.

(11) Urahata, S. M.; Ribeiro, M. C. C. Structure of Ionic Liquids of 1-Alkyl-3-Methylimidazolium Cations: A Systematic Computer Simulation Study. *J. Chem. Phys.* **2004**, *120*, 1855–1863.

(12) Wang, Y.; Voth, G. A. Unique Spatial Heterogeneity in Ionic Liquids. *J. Am. Chem. Soc.* **2005**, *127*, 12192–12193.

(13) Bhargava, B. L.; Devane, R.; Klein, M. L.; Balasubramanian, S. Nanoscale Organization in Room Temperature Ionic Liquids: A Coarse Grained Molecular Dynamics Simulation. *Soft Matter* **2007**, *3*, 1395–1400.

(14) Lopes, J.; Padua, A. Nanostructural Organization in Ionic Liquids. *J. Phys. Chem. B* **2006**, *110*, 3330–3335.

(15) Gomes, M. F. C.; Lopes, J. N. C.; Padua, A. A. H. Thermodynamics and Micro Heterogeneity of Ionic Liquids. *Top. Curr. Chem.* **2009**, *290*, 161–183.

(16) Hardacre, C.; Holbrey, J. D.; Mullan, C. L.; Youngs, T. G. A.; Bowron, D. T. Small Angle Neutron Scattering from 1-Alkyl-3-Methylimidazolium Hexafluorophosphate Ionic Liquids ([C(N)Mim]-[PF_6], N=4, 6, and 8. *J. Chem. Phys.* **2010**, *133*, 074510.

(17) Annapureddy, H. V. R.; Kashyap, H. K.; De Biase, P. M.; Margulis, C. J. What Is the Origin of the Prepeak in the X-ray Scattering of Imidazolium-Based Room-Temperature Ionic Liquids? *J. Phys. Chem. B* **2010**, *114*, 16838–16846.

(18) Sarkar, A.; Trivedi, S.; Baker, G. A.; Pandey, S. Multiprobe Spectroscopic Evidence for "Hyperpolarity" within 1-Butyl-3-Methylimidazolium Hexafluorophosphate Mixtures with Tetraethylene Glycol. *J. Phys. Chem. B* **2008**, *112*, 14927–14936.

(19) Guo, J.; Baker, G.; Hillesheim, P. C.; Dai, S.; Shaw, R. W.; Mahurin, S. M. Fluorescence Correlation Spectroscopy Evidence for Structural Heterogeneity in Ionic Liquids. *Phys. Chem. Chem. Phys.* **2011**, *13*, 12395–12398.

(20) Funston, A. M.; Fadeeva, T. A.; Wishart, J. F.; Castner, E. W., Jr. Fluorescence Probing of Temperature-Dependent Dynamics and Friction in Ionic Liquid Local Environments. *J. Phys. Chem. B* **2007**, *111*, 4963–4977.

(21) Fruchey, K.; Fayer, M. D. Dynamics in Organic Ionic Liquids in Distinct Regions Using Charged and Uncharged Orientational Relaxation Probes. *J. Phys. Chem. B* **2010**, *114*, 2840–2845.

(22) Xiao, D.; Rajian, J. R.; Cady, A.; Li, S.; Bartsch, R. A.; Quitevis, E. L. Nanostructural Organization and Anion Effects on the Temperature Dependence of the Optical Kerr Effect Spectra of Ionic Liquids. *J. Phys. Chem. B* **2007**, *111*, 4669–4677.

(23) Xiao, D.; Rajian, J. R.; Hines, L. G., Jr.; Li, S.; Bartsch, R. A.; Quitevis, E. L. Nanostructural Organization and Anion Effects in the Optical Kerr Effect Spectra of Binary Ionic Liquid Mixtures. *J. Phys. Chem. B* **2008**, *112*, 13316–13325.

(24) Xiao, D.; Rajian, J. R.; Li, S.; Bartsch, R. A.; Quitevis, E. L. Additivity in the Optical Kerr Effect Spectra of Binary Ionic Liquid Mixtures: Implications for Nanostructural Organization. *J. Phys. Chem. B* **2006**, *110*, 16174–16178.

(25) Turton, D. A.; Hunger, J.; Stoppa, A.; Hefter, G.; Thoman, A.; Walther, M.; Buchner, R.; Wynne, K. Dynamics of Imidazolium Ionic Liquids from a Combined Dielectric Relaxation and Optical Kerr Effect Study: Evidence for Mesoscopic Aggregation. *J. Am. Chem. Soc.* **2009**, *131*, 11140–11146.

(26) Yang, P.; Voth, G. A.; Xiao, D.; Hines, L. G.; Bartsch, R. a.; Quitevis, E. L. Nanostructural Organization in Carbon Disulfide/Ionic Liquid Mixtures: Molecular Dynamics Simulations and Optical Kerr Effect Spectroscopy. *J. Chem. Phys.* **2011**, *135*, 034502.
(27) Nicolau, B. G.; Sturlaugson, A.; Fruchey, K.; Ribeiro, M. C. C.; Fayer, M. D. Room Temperature Ionic Liquid-Lithium Salt Mixtures: Optical Kerr Effect Dynamical Measurements. *J. Phys. Chem. B* **2010**, *114*, 8350−8356.
(28) Sturlaugson, A. L.; Fruchey, K. S.; Fayer, M. D. Orientational Dynamics of Room Temperature Ionic Liquid/Water Mixtures: Evidence for Water-Induced Structure and Anisotropic Cation Solvation. *J. Phys. Chem. B* **2012**, *116*, 1777−1787.
(29) Mizoshiri, M.; Nagao, T.; Mizoguchi, Y.; Yao, M. Dielectric Permittivity of Room Temperature Ionic Liquids: A Relation to the Polar and Nonpolar Domain Structures. *J. Chem. Phys.* **2010**, *132*, 164510.
(30) Imanari, M.; Uchida, K. I.; Miyano, K.; Seki, H.; Nishikawa, K. NMR Study on Relationships between Reorientational Dynamics and Phase Behaviour of Room-Temperature Ionic Liquids: 1-Alkyl-3-Methylimidazolium Cations. *Phys. Chem. Chem. Phys.* **2010**, *12*, 2959−2967.
(31) Chiappe, C. Nanostructural Organization of Ionic Liquids: Theoretical and Experimental Evidences of the Presence of Well Defined Local Structures in Ionic Liquids. *Monatsh. Chem.* **2007**, *138*, 1035−1043.
(32) Russina, O.; Triolo, A.; Gontrani, L.; Caminiti, R.; Xiao, D.; Hines, L. G. J.; Bartsch, R. A.; Quitevis, E. L.; Pleckhova, N.; Seddon, K. R. Morphology and Intermolecular Dynamics of 1-Alkyl-3-Methylimidazolium Bis(Trifluoromethane)Sulfonylamide Ionic Liquids: Structural and Dynamic Evidence of Nanoscale Segregation. *J. Phys.: Condens. Matter* **2009**, *21*, 424121.
(33) Atkin, R.; Warr, G. G. The Smallest Amphiphiles: Nanostructure in Protic Room-Temperature Ionic Liquids with Short Alkyl Groups. *J. Phys. Chem. B* **2008**, *112*, 4164−4166.
(34) Xiao, D.; Hines, L. G.; Bartsch, R. A.; Quitevis, E. L. Intermolecular Vibrational Motions of Solute Molecules Confined in Nonpolar Domains of Ionic Liquids. *J. Phys. Chem. B* **2009**, *113*, 4544−4548.
(35) Pádua, A. A. H.; Costa Gomes, M. F.; Canongia Lopes, J. N. A. Molecular Solutes in Ionic Liquids: A Structural Perspective. *Acc. Chem. Res.* **2007**, *40*, 1087−1096.
(36) Fruchey, K.; Lawler, C. M.; Fayer, M. D. Investigation of Nanostructure in Room Temperature Ionic Liquids Using Electronic Excitation Transfer. Supporting Information. *J. Phys. Chem. B* **2012**, *116*, 3054−3064.
(37) Hanke, C. G.; Johansson, A.; Harper, J. B.; Lynden-Bell, R. M. Why Are Aromatic Compounds More Soluble Than Aliphatic Compounds in Dimethylimidazolium Ionic Liquids? A Simulation Study. *Chem. Phys. Lett.* **2003**, *374*, 85−90.
(38) Harper, J. B.; Lynden-Bell, R. M. Macroscopic and Microscopic Properties of Solutions of Aromatic Compounds in an Ionic Liquid. *Mol. Phys.* **2004**, *102*, 85−94.
(39) Blesic, M.; Lopes, J. N. C.; Padua, A. A. H.; Shimizu, K.; Gomes, M. F. C.; Rebelo, L. P. N. Phase Equilibria in Ionic Liquid-Aromatic Compound Mixtures, Including Benzene Fluorination Effects. *J. Phys. Chem. B* **2009**, *113*, 7631−7636.
(40) Wirth, P.; Schneider, S.; Dörr, F. S1-Lifetimes of Triphenylmethane and Indigo Dyes Determined by 2-Photon-Fluorescence Technique. *Opt. Commun.* **1977**, *20*, 155−158.
(41) Chuang, T. J.; Eisenthal, K. B. Theory of Fluorescence Depolarization by Anisotropic Rotational Diffusion. *J. Chem. Phys.* **1972**, *57*, 5094−5097.
(42) Xu, J.; Shen, X.; Knutson, J. R. Femtosecond Fluorescence Upconversion Study of the Rotations of Perylene and Tetracene in Hexadecane. *J. Phys. Chem. A* **2003**, *107*, 8383−8387.
(43) Sension, R. J.; Hochstrasser, R. M. Comment On: Rotational Friction Coefficients for Ellipsoids and Chemical Molecules with Slip Boundary Conditions. *J. Chem. Phys.* **1993**, *98*, 2490−2490.
(44) Fury, M.; Jonas, J. Molecular Reorientation and Shear Viscosity in Dense Liquids. *J. Chem. Phys.* **1976**, *65*, 2206−2210.
(45) Youngren, G. K.; Acrivos, A. Rotational Friction Coefficients for Ellipsoids and Chemical Molecules with the Slip Boundary Condition. *J. Chem. Phys.* **1975**, *63*, 3846−3848.
(46) Hu, C.-M.; Zwanzig, R. Rotational Friction Coefficients for Spheroids with the Slipping Boundary Condition. *J. Chem. Phys.* **1974**, *60*, 4354−4357.
(47) Wirth, M. J.; Chou, S. H. Behavior of the Rotational Diffusion Tensor of Tetracene under Subslip Conditions. *J. Phys. Chem.* **1991**, *95*, 1786−1789.
(48) Kim, Y. R.; Hochstrasser, R. M. Rotational Diffusion of Fluorene in Hydroxylic Solvents. *J. Phys. Chem.* **1992**, *96*, 9595−9597.
(49) Blanchard, L. A.; Gu, Z.; Brennecke, J. F. High-Pressure Phase Behavior of Ionic Liquid/CO_2 Systems. *J. Phys. Chem. B* **2001**, *105*, 2437−2444.
(50) Méndez-Morales, T.; J., C.; Bouzón-Capelo, S.; Pérez-Rodríguez, M.; Cabeza, Ó.; Gallego, L. J.; Varela, L. M. MD Simulations of the Formation of Stable Clusters in Mixtures of Alkaline Salts and Imidazolium-Based Ionic Liquids. *J. Phys. Chem. B* **2013**, *117*, 3207−3220.
(51) Tiwari, S.; Khupse, N.; Kumar, A. Intramolecular Diels-Alder Reaction in Ionic Liquids: Effect of Ion-Specific Solvent Friction. *J. Org. Chem.* **2008**, *73*, 9075−9083.